Molecular Organization of the Cholesteryl Ester Droplets in the Fatty Streaks of Human Aorta

DONALD M. ENGELMAN and GERALD M. HILLMAN

From the Department of Molecular Biophysics and Biochemistry, Yale University, New Haven, Connecticut 06520

ABSTRACT X-ray diffraction patterns from human arterial specimens containing atherosclerotic fatty streak lesions exhibited a single sharp reflection, corresponding to a structural spacing of about 35 Å. Specimens without lesions did not. When specimens with fatty streaks were heated, an order-to-disorder phase transition was revealed by the disappearance of the sharp reflection. The transition was thermally reversible and its temperature varied from aorta to aorta over a range from 28° to 42°C. Since cholesteryl ester droplets are a major component of fatty streaks, comparison studies were made of the diffraction behavior from pure cholesteryl esters. We found that the diffraction patterns of the fatty streak material could be accounted for by the organization of the cholesteryl esters into a liquid-crystalline smectic phase that melts from the smectic to a less ordered phase upon heating.

When combined with the conclusions of others from polarized light microscopy, our study shows that a droplet in the smectic phase has well-defined concentric layers of lipid molecules. In each layer, the long axes of the molecules have a net radial orientation with respect to the droplet, but the side-to-side organization is disordered. We suggest that the accessibility of portions of the lipids for specific binding to enzymes or transport proteins may be restricted when they are in the smectic state, and that exchange of lipids with surrounding membranes or other potential binding sites may likewise be inhibited. The restriction in the smectic phase should be greater than in the less ordered phases that exist at higher temperatures.

This work was part of the doctoral thesis of G. M. Hillman (1), and part of this work has been reported previously in an abstract (2).

Received for publication 10 October 1975 and in revised form 28 June 1976.

INTRODUCTION

Many atherosclerotic lesions are characterized by an accumulation of lipid in the intimal layer of the aorta. The molecular mechanisms of lipid accumulation are poorly understood, but examinations of the physical-chemical properties of lipid deposits have revealed properties that may affect the process of accumulation. It has been shown that the organization of lipid deposits in a wide range of lesions can be accounted for by lipid-lipid interactions alone (3). Thus, lipid droplets that consist almost entirely of cholesteryl esters have been found in fatty streak lesions (4). These droplets, 0.5–5 μm in diameter, comprise most of the accumulated lipid in fatty streak lesions. Microscopists have observed that many of the droplets are birefringent (3–6) and Hata et al. (7) attempted to characterize droplet molecular structure by optical crystallography. They proposed several different models for the organization of cholesteryl ester molecules in the droplet which could account for their optical characteristics but which were indistinguishable by optical techniques. The purpose of our study is to determine the structure of the droplets by an independent technique capable of distinguishing between the models proposed by Hata et al.

Pure cholesteryl esters are known to exist in liquid-crystalline mesophases; that is, states less ordered than crystalline states but more ordered than a pure liquid state (see ref. 8 and 9). Fig. 1 depicts the molecular organization of the different thermotropic states of a commonly found cholesteryl ester. The structural differences between esters organized in the smectic mesophase and those in the less ordered nematic, cholesteric, or liquid phases may be the basis for the accumulation and persistence of some lipid deposits and the catabolism and regression of others. An ability

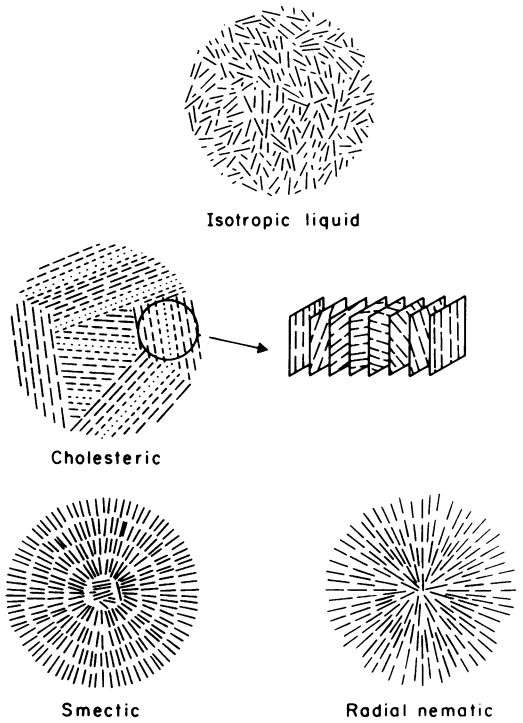

FIGURE 1 Physical states of cholesteryl ester droplets. A cholesteryl ester, when extended, is a rod-like molecule. It is depicted here as a line segment. There is no apparent long-range organization in the liquid phase. In the cholesteric phase the molecules line up end-to-end and in a given plane the lines are parallel but the ends of the molecules are not in alignment. As one moves from plane to plane the direction of the lines shifts incrementally, producing a progressive twist in the molecular orientations. Cholesteric droplets appear to consist of several small domains of molecules organized in the cholesteric state. In the radial nematic phase, the molecules line up end-to-end with their long axes lying on the radial vector. Molecules lying on adjacent radial vectors would not be in alignment. The molecules in the smectic phase are packed into periodically spaced shells 34 Å thick (which, from the point of view of a molecule, is a planar lamella). The droplet consists of concentrically packed shells somewhat like layers of an onion. Within each lamella, the side-to-side packing of the molecules is liquid-like, and long-range periodicities are absent. Note that the ends of the molecules are more or less aligned. Droplets having smectic or radial nematic organization would be indistinguishable by their appearance in the polarizing microscope; however, X-ray diffraction measurements distinguish between these two alternatives.

to identify the state of the lipids in the lesion will be necessary for the consideration of this possibility.

X-ray diffraction is a sensitive measure of periodic structures at the molecular level. Cholesteryl ester molecules organized in the smectic state (Fig. 1) give a characteristic X-ray scattering pattern that reveals the existence of the periodic smectic lamellae, the size or extent of order of the diffracting structure, the dimensions of the periodic unit (i.e., the lamellar thickness), and information concerning the electron density within the repeat unit. The crystalline phase and the liquid-crystalline smectic mesophase of cholesteryl esters have readily distinguishable X-ray diffraction patterns. Nematic, cholesteric, and liquid states, while distinct from the smectic and crystal phases, are difficult to distinguish from each other. Thus, X-ray diffraction measurement can readily distinguish among three alternative states: the crystalline phase, the smectic phase, and less ordered phases.

In this paper, we present findings based on the application of X-ray diffraction methods to studies of human fatty streak lesions that combine with the polarized light observation to define the general molecular organization of the strongly birefringent droplets. Pure phases of cholesteryl esters were also examined as models for the behavior of the fatty streak material. This work has been presented previously in preliminary form (2). The demonstration that the droplets of the fatty streak deposit are organized in a smectic mesophase that changes thermotropically to a less ordered state confirms the tentative conclusion of Hata et al. (7). Possible implications for the process of lipid accumulation are discussed.

METHODS

Source of material. Human aorta specimens were taken at autopsy within 24 h after death. Because we were interested in fatty streak lesions, predominately found in younger people, most aortas were obtained from subjects between the ages of 15 and 40 yr. Specimens from subjects who died from diseases thought to complicate atherosclerosis (such as diabetes) were rejected. The age, sex, and cause of death of each individual from whom a specimen was taken is given in Table I. A 3–6-inch piece of human aorta was immersed in buffer A[1] and stored at 4°C for no more than a day.

Fatty streak morphology. When an aorta is cut open longitudinally, the atherosclerotic lesions are visible on the lumenal surface. We identified lesion types initially by their gross appearance (10). Later, the identification was confirmed histologically (see below).

"Normal" tissue is defined as tissue lacking visible lesions. From the lumenal side, normal tissue is pinkish-white. The surface is smooth and flat; it is soft in texture. Lesions appear as distinct entities on the normal tissue surface.

Several visible morphological features of lesions were applied in identifying fatty streaks. Fatty streaks are (*a*) yellowish; (*b*) variable in size (some are barely visible and some are long, thin patches 5 × 2 mm); (*c*) located parallel to the length of the aorta, primarily in the vicinity of the line connecting the many pairs of arteries that lead from the aorta; (*d*) usually flat at the endothelial surface, although in more advanced fatty streaks the endothelial surface may be slightly raised; (*e*) contiguous and smooth or speckled and bumpy (however, in both cases they were soft in texture). Most aortas selected for this study con-

[1] Buffer A: 0.155 M NaCl and 0.1 M Na_2PO_4 titrated to pH 7.4 with HCl.

TABLE I

X-Ray Diffraction of Human Fatty Streaks

Aorta specimen	Age	Sex	Cause of death	Histology	Bragg spacing	Transition temperature
	yr				*Å*	*°C*
1	35	M	Fractured skull		35.0	31
2	20	M	Multiple thrombo-embolism and thrombocytosis		35.6	<34
3	25	F	Leukemia		35.9	35
4	21	F	Breast cancer		35.5	37.5
5a	20	M	Auto accident	X	36.8	38.5±1.5
b				X	36.4	38.5±1.5
6	42	M	Myocardial infarct	X	34.8	38.5±1.5
7	37	F	Breast cancer		36.0	38.5±1.5
8	34	F	Laennec's cirrhosis	X	36.8	—
9	43	M	Lymphoma		35.3	40.5±3.5
10	19	M	Strangulation		36.5	38.7±1.2
11	23	M	Gunshot	X	35.2	—
12	19	F	Smoke inhalation	X	34.5	38
13a	17	M	Pulmonary edema	X	36.7	—
b			(possible suicide)	X	35.2	39
14	30	F	Gunshot	X	36.4	39
15	20	M	Cancer of testis	X	36.0	40±1
16	24	M	Smoke inhalation		36.1	41.1±2.1
17	36	F	Plane crash	X	35.7	—
18	28	F	Unknown		36.1	40
19a	26	F	Auto accident	X	35.0	40
b				X	35.8	40
20	35	M	Gunshot		35.9	—

Aorta specimens from autopsy were dissected to remove intima-media strips containing fatty streak lesions. X-ray diffraction experiments were conducted at various temperatures to observe changes in the state of the lipids in the deposits. In each case where a range of temperatures is indicated, the lower temperature is the last point at which the characteristic, low-angle diffraction peak was seen, and the upper temperature is the next experimental point above that temperature, so the high temperature limit for this phase transition lies between the indicated temperatures. In cases where the range is known to within 1°C only the intermediate temperature is given. The samples which were examined histologically are indicated. In this data, age, sex, equivalent Bragg spacing of the smectic reflection, and the smectic melting temperature are not correlated. Perhaps in a larger sample size, with the specimens categorized according to sex, age, both weight, and cause of death Bragg spacings and melting temperatures will correlate.

tained predominately fatty streaks as opposed to other lesions.

More advanced lesions have a different appearance. Fibrous plaques are (*a*) yellowish gray or pearly white; (*b*) often larger than fatty streaks; (*c*) not located in all the places fatty streaks are; (*d*) elevated above the endothelial surface; (*e*) often gristly in texture. Complicated lesions evolve from fibrous plaques. Many complicated lesions can be recognized macroscopically because they have become ulcerated or they have become calcified and hardened. Aortas that contained advanced lesions were not included in this study.

The intima-media preparation. Samples for X-ray diffraction experiments were prepared as follows: An area around a visible fatty streak was outlined (~ 1–2 × 3–4 mm) by a shallow cut from a razor blade. The thin layer of tissue (~ 150 μm deep) enclosed by the cut was then gently peeled off from the lumenal side and immersed in buffer A. This piece of tissue contained the endothelial layer, the intima, and a few medial layers. It also contained the visible lesion. A sample prepared this way is termed an intima-media preparation. Intima-media preparations were also made from regions with no visible lesions for use as controls in X-ray diffractoin experiments.

Histology. Two small rectangular blocks were cut from tissue containing visible fatty streaks. The blocks were adjacent to areas from which intima-media preparations were excised for X-ray experiments. Fixed overnight in a fresh 3% formalin solution of buffer A, frozen sections were prepared from one block and paraffin-embedded sections were prepared from the other. The frozen sections were stained for lipid with Oil Red O (E. I. du Pont de Nemours

& Co., Wilmington, Del.) (11) and the paraffin-embedded sections were stained for cell nuclei with hematoxylin and counterstained with eosin.

Several morphological features defined the fatty streak microscopically. The intima was thickened in tissue that contained fatty streak lesions. There were many Oil Red O-stained droplets, often aggregated into clusters in the intima, and in a few cases Oil Red O-stained droplets were observed as deep as the first few cell layers of the media. No structure in the middle or deep media or in the adventitia was stained by Oil Red O. In most cases there was no medial involvement; however, occasionally, a few medial cell layers adjacent to the internal elastic lamina were disrupted. No fibrosis was observed. Many hematoxylin-stained cell nuclei were observed in intimal layers containing fat deposits. Specimens were rejected from the study if they contained lesions in which fibrosis had occurred. Fatty streak lesions were confirmed histologically under the microscope for a majority of the specimens investigated. Specimens examined histologically are indicated in Table I.

The X-ray apparatus. A Picker 80-000 multifocus X-ray generator unit (Jarrel Ash Div., Fisher Scientific Co., Waltham, Mass.) was used with a copper target (Cu Kα radiation). An Elliott toroidal-point focusing camera (Searle Co., London, England) was used to focus the X-ray beam (12). For a few studies a Franks camera (13) was used instead. With both cameras, the diffraction patterns were recorded on film. During an exposure, the camera was evacuated to minimize gas scatter.

Sample preparation. Intima media preparations were suspended in buffer A and sealed in thin-walled (1.0 mm outside diameter) glass capillaries (Pantak, West Germany, distributed by Uni-Mex Co., Griffith, Ind.). Capillaries were then placed in the thermally controlled specimen holder for the experiment. The holder consisted of a brass block regulated by a circulating water bath. The block was in intimate contact with the X-ray capillary immediately adjacent to the X-ray beam, and calibration experiments demonstrated regulation to ±0.5°C (1).

The X-ray diffraction thermal scan. The protocol for data collection was as follows: First, the center of the X-ray beam was recorded, and the thermal control was set to a given temperature (usually to 37°C, for the initial point of a temperature scan). When the bath had reached that temperature, 20 min was allowed for the system to come to thermal equilibrium and then the exposure was begun. Exposures of more than 18–24 h did not reveal any additional features of the diffraction pattern, and the principal low-angle reflection from a suitable intima-media preparation could be obtained in as little as 4–6 h. The diffraction patterns and phase behavior exhibited by intima-media preparations at the beginning of an experiment were indistinguishable from the patterns and phase behavior observed for up to 10 days later. The initial information obtained from the film was whether the principal low-angle reflection was present. If it was, the temperature of the system was increased for the next picture. If it was not, the temperature was lowered for the next picture. In our early studies we wished to demonstrate a reversible phase transition. Thus the temperature interval was large, sometimes as high as 10° C. In later studies our temperature scans became more systematic and temperature points were taken every degree, starting at 37°C and incrementing in the direction of the phase transition.

If a Bragg reflection was observed at 37°C but had disappeared at 39.0°C, then the transition temperature would lie in that interval. The transition temperature would be reported in Table I as (38.0±1.0)°C. On an absolute scale we would know that the transition occurred between 36.5 and 39.5°C. On a relative scale, temperature differences of 0.1–0.2°C are significant. Differences in transition temperatures are meaningful if their transition intervals do not overlap. If two intervals do not overlap but are not separated by more than 0.2°C, there is a slight possibility that the transition temperature would be the same. However, if the two intervals are separated by more than 0.2°C, a transition temperature difference is confidently defined.

Chemical analysis. The chemical analysis of the lipid in the lesion followed the procedure of Lang and Insull (4) closely. Intima-media preparations containing lesions were placed in 5 ml of buffer A, minced with a scalpel, and homogenized in a tissue grinder. This released intracellular and extracellular lipid droplets from the tissue. The resultant mixture of lipid droplets, buffer A, and tissue was then centrifuged at 10 *g* and 4°C for about 45 min. Three regions emerged: a lower pellet containing cell membranes and connective tissue, a clear supernate, and a floating layer containing the lipid droplets. The floating layer was the region of interest. It was removed for chemical analysis.

Cholesteryl esters were separated from free cholesterol, phospholipids, and triglycerides by thin layer chromatography (TLC) by the approach of Lang and Insull (4). The floating (lipid-containing) layer was dissolved in a 75:25 chloroform-hexane solution, spotted on a 15-cm-square silica gel HR plate (Analtech, Inc., Newark, Del.), and developed with 80:20 benzene-acetone solution. The method clearly separated cholesteryl esters from the other classes of lipid. The lipid composition of fatty streak lesions from four aortas was estimated from sulfuric acid-charred spots. The results for each case was in agreement with Lang and Insull (4), showing that the major class of lipid is cholesteryl ester (> 85%). The cholesteryl ester spot from a heavily loaded plate was scraped off and methyl esters of fatty acids from one specimen were prepared by a boron trifluoride-methanol treatment (14). Gas-liquid chromatography analysis of the fatty acid methyl esters showed that the major esters were cholesteryl oleate (37%), cholesteryl linoleate (10%), and cholesteryl palmitate (18%). These analyses were conducted to verify that the major lipid components in our droplets were cholesteryl esters and to ascertain that the cholesteryl ester fatty acid spectrum of our droplets was similar to that reported in Lang and Insull's exhaustive study (4).[2]

It would have been interesting to correlate the transition temperatures and Bragg spacings measured by X-ray diffraction from fatty streak material with chemical composition data; however, such a correlation was not possible in this study. The X-ray beam samples only a small amount of the cholesteryl ester deposits found in the intima-media preparation. The beam is about 1 mm in extent along the 0.7-mm-diameter capillary (which contains the specimen). Thus the beam samples a maximum of 0.4 mm^3 of tissue. From an analysis of photomicrographs of intima containing fatty inclusions, we found that droplets occupy a maximum of 3% of the tissue by volume, and generally much less. Thus a 0.4 mm^3 piece of tissue will contain less than 0.01 mg of cholesteryl esters. This minute quantity of cholesteryl esters must be separated from the tissue and from other lipids. Then the fatty acids must be de-esterified from the cholesterol moiety and re-esterified to methyl groups for

[2] Cholesteryl oleate (50%), cholesteryl linoleate (15%), and cholesteryl palmitate (9%). (4).

fatty acid analysis by GLC. The losses incurred during the isolation procedures make this study difficult. The inability to determine and excise the exact piece of tissue through which the beam passed make this study even less feasible. That such precision is necessary to correlate melting and spacing data with chemical composition data is shown by the melting point heterogeneity in human fatty streak material (15). Droplets 1 μm in diameter (observed within a 100 μm^2 field) vary in melting temperature by as much as 10–15°C, which is most directly explained as arising from differences in their chemical composition.

The model system studies. Diffraction patterns as a function of temperature were recorded for pure (99%, determined by gas-liquid chromatography) cholesteryl myristate, cholesteryl oleate, and cholesteryl linoleate (purchased from Analabs, Inc., subsidiary of New England Nuclear Corp., North Haven, Conn.). Care was taken to minimize oxidative degradation due to air contact, and a control experiment using thin-layer and gas liquid chromatography analyses showed no oxidation of the specimen after the X-ray experiments, as judged by the appearance of lyso compounds, free fatty acids, and oxidized fatty acids.

RESULTS

X-ray studies on atherosclerotic material. X-ray diffraction patterns obtained from intima-media preparations containing fatty streaks exhibited a sharp, intense, (36 Å)$^{-1}$ Bragg reflection at low temperatures (see Fig. 2*b*). The reflection was the strongest feature of the pattern and was clearly visible above the background noise. No other Bragg reflections were observed with the toroid camera in the range from (107 Å)$^{-1}$ to (3.1 Å)$^{-1}$, even though the method could detect reflections 1,000 times weaker than the (36 Å)$^{-1}$ peak. Low-temperature patterns were also obtained with the Franks camera, which allowed better low-angle resolution than the toroid camera. The weak beam intensity and long exposure time permitted a recording sensitivity down to only one-fifth the intensity of the principal reflection. Nevertheless, no other reflections were observed to (471 Å)$^{-1}$, and we conclude that the observed reflection is the first order.

Intima-media preparations containing fatty streaks from 20 aortas were examined with X-ray diffraction. At low temperatures, every specimen exhibited the characteristic single sharp peak near (36 Å)$^{-1}$, although there was some variation in spacing. Because the (36 Å)$^{-1}$ reflection was sharp, the periodic order of the structure giving rise to the reflection must have extended over a long range. A Debye-Scherrer calculation from the peak width (16) indicates that the coherently diffracting regions are more than 500 Å in extent. As the specimen was heated, the peak intensity began to fall. For the specimen studied in Fig. 2, the peak was invisible by 37.5°C (see Fig. 2*a*). The peak reappeared on cooling. The Bragg reflection demonstrates the presence of a periodically ordered structure, and its disappearance shows a loss of order due to a thermotropic order-to-disorder phase transition. The phase transition was observed in every thermal scan, and the temperature at which the peak disappeared varied from aorta to aorta over the range from 28°C to 42°C. The data are summarized in Table I. The temperature range over which the peak progressively weakened defined the width of the transition, which for most specimens was about 5–10°C.

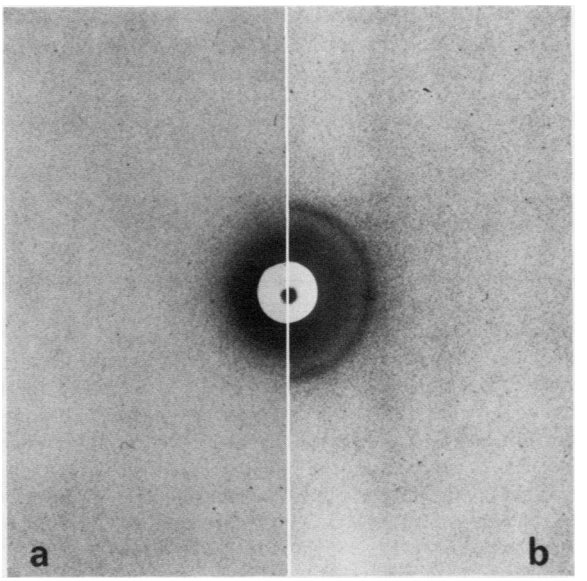

FIGURE 2 Diffraction from an intima-media preparation from human aorta containing fatty streaks. Regions of the intima containing macroscopic fatty streaks were dissected from an affected aorta and sealed in a glass capillary. X-ray exposures were made as a function of temperature, with a point-focusing camera. The portions of the patterns shown here extend from about (100 Å)$^{-1}$ equivalent Bragg spacing (next to the beam stop) to about (7 Å)$^{-1}$ at the edge of the print, though we observed them out to (3 Å)$^{-1}$. The diffraction near the beam stop evident in both *a* and *b* is considered to be scattering from material other than the fatty droplets (compare Fig. 3). (*a*) the preparation at 37°C. (*b*) the preparation at 27°C. Note the strong, sharp line at (36 Å)$^{-1}$ present at the lower temperature.

To demonstrate that the (36 Å)$^{-1}$ peak arose from structures in the fatty streak lesion, intima-media preparations from normal areas were studied with X-ray diffraction. The (36 Å)$^{-1}$ reflection was not observed and, indeed, no other Bragg reflections were found, even when the temperature was dropped to 4°C.

An attempt was made to establish the origin of the (36 Å)$^{-1}$ peak directly. Some of the droplets isolated for chemical analysis were examined by X-ray diffraction. One sample exhibited the characteristic (36 Å)$^{-1}$ peak and had a reversible phase transition near 37°C; however, it also exhibited several wide-angle reflections near (4 Å)$^{-1}$, which were not observed in diffrac-

TABLE II

Smectic Melting Temperatures and Characteristic Smectic Peak Spacing for Three Cholesteryl Esters

	Tm*	Tm‡	Spacing§
	°C	°C	Å
Cholesteryl myristate	85.5	85.5±1	33.5‖
Cholesteryl oleate	40.5	39±2	33.7¶
Cholesteryl linoleate	30.0	34.5	35.2**

* Smectic-cholesteric transition temperature determined by polarized light microscopy.

‡ Smectic less-ordered phase transition temperature determined by X-ray diffraction. If a range is indicated for the transition point, the lower temperature is the highest temperature at which the sharp, characteristic low-angle smectic peak was observed, and the higher temperature is the lowest temperature in which the line was not observed. In cases where the range is known to within 1°C, only the midpoint temperature is reported.

§ Equivalent Bragg spacing of the characteristic smectic reflection.

‖ Observed at 82°C.

¶ Observed at 37°C.

** Observed at 32°C.

tion patterns from intima-media preparations containing fatty streak lesions. The results suggest that some crystallization occurred in the sample during the isolation process and that perhaps the diffraction pattern we obtained arose from a mixture of smectic droplets and crystals. Therefore we decided to confine our investigation to the structure of the droplets *in situ*. Although crystals were present, the isolation experiment serves as a positive control to establish that the isolated droplets contain the material giving rise to the diffraction we observed.

The diffraction patterns of preparations both with and without fatty streaks exhibited a considerable amount of diffuse scatter. Most of it was concentrated in three regions. First, there was diffuse scatter near the central beam. Second, there was a broad, diffuse band in the wide-angle region, centered between (10 Å)$^{-1}$ and (14 Å)$^{-1}$, depending on the sample. Finally, there was diffuse scatter beginning at about (5.5 Å)$^{-1}$ and extending to the edge of the film [about (3 Å)$^{-1}$]. Unlike the (36 Å)$^{-1}$ peak, the diffuse bands did not change much with temperature in the range from 4°C to 45°C. This supports the notion that much of the diffuse scatter arose from structures in the tissue other than the one giving rise to the (36 Å)$^{-1}$ Bragg reflection.

The model studies. Pure synthetic cholesteryl myristate, cholesteryl oleate, and cholesteryl linoleate were observed with a thermally controlled polarized light microscope and a quarter-wave plate in each of their

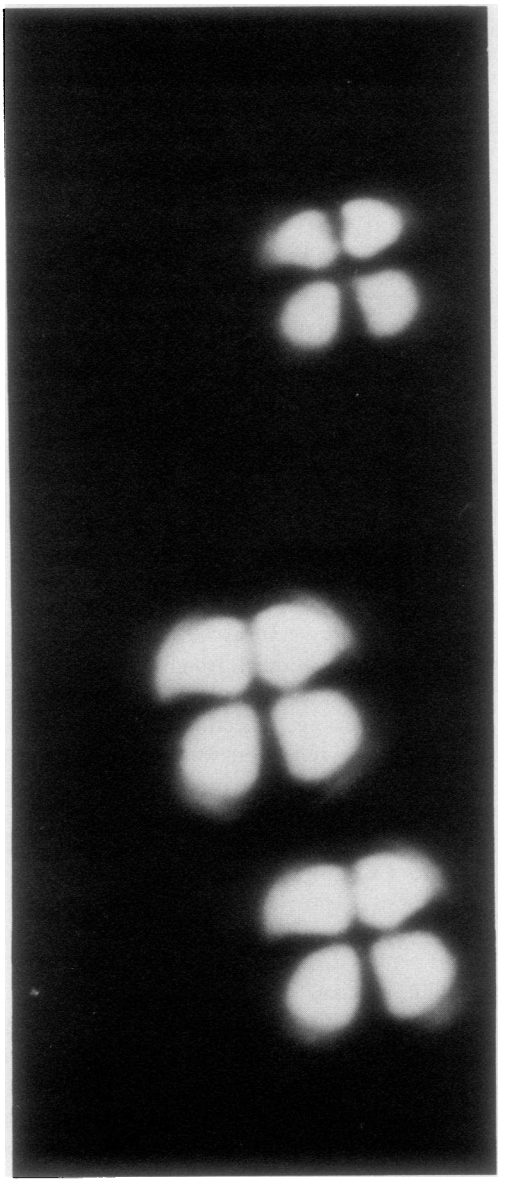

FIGURE 3 Droplets exhibiting the formée cross. A mixture of water : cholesteryl oleate : phosphatidyl serine : 97.5 : 2.5 : 0.25 was sonicated under N_2 at 35°C for 30 min in a bath sonicator (G. G. Shipley, personal communication). Spherical droplets were formed that maintained their integrity for long periods without fusing with each other. The droplets exhibit the phase behavior seen in bulk phases of cholesteryl oleate. The droplets shown are about 10 μm in diameter and exhibit the formée cross in the polarizing microscope. When viewed with a quarter-wavelength plate, the color pattern corresponds to a positive sign of birefringence. These observations demonstrate the presence of a radially enhanced polarizability, which may arise from a smectic or radial nematic liquid crystal mesophase. X-ray measurements of the preparation show the characteristic diffraction pattern of the smectic phase, which permits positive identification of the general organization of the droplets. The photograph was taken at 37.7°C.

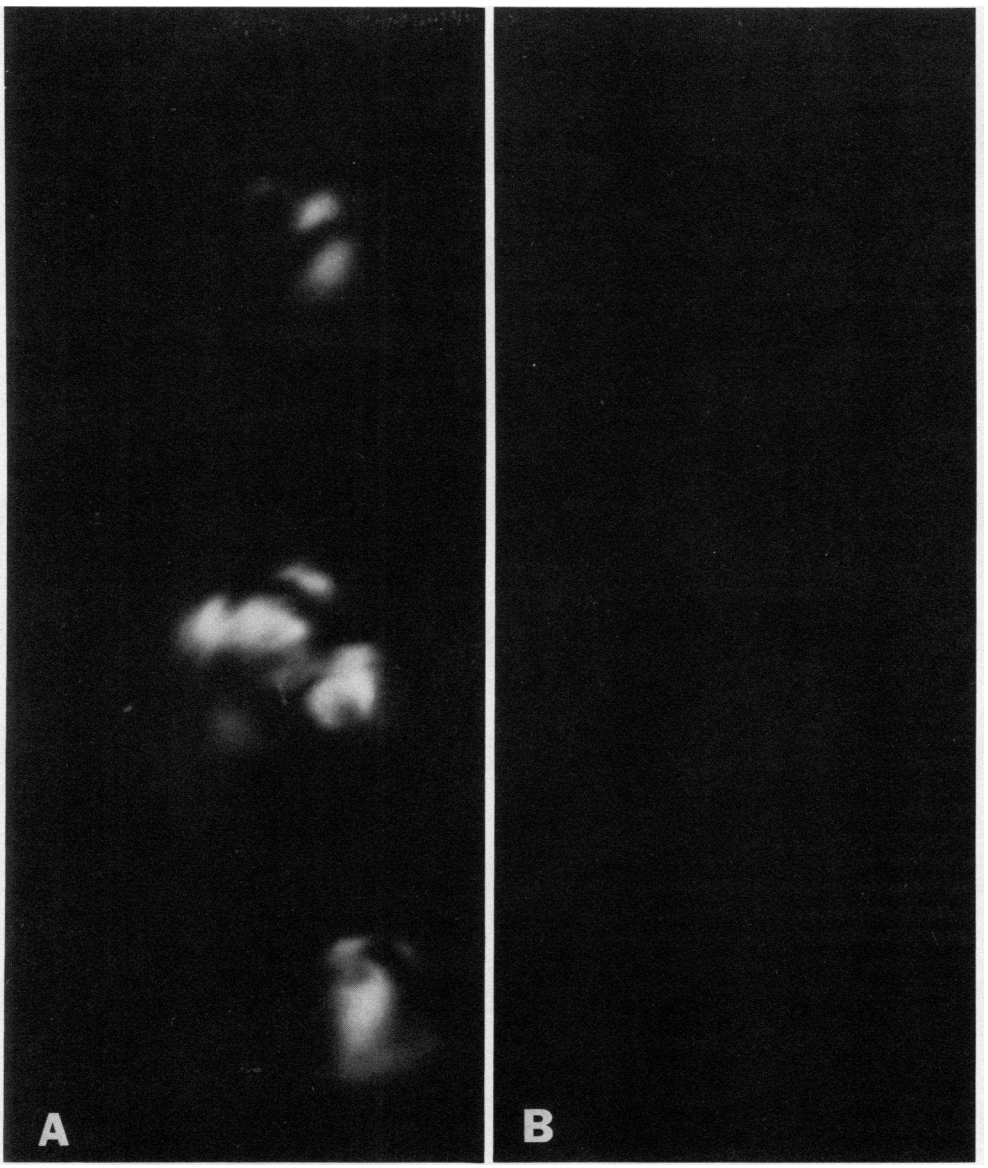

FIGURE 4 Cholesteric and isotropic droplets. The droplet preparation shown in Fig. 3 was heated and two changes in the image were seen in the polarized light microscope. At 39.0° the formée cross image was replaced by the mottled birefringence seen in Fig. 4A (39.0°C), which we interpret as a distorted cholesteric phase. As the temperature is raised above 43.5°C, the birefringence disappears as the droplets become isotropic (Fig. 4B, 43.6°C). The transition temperatures observed in the droplets appear to be shifted approximately 1° down from those seen in bulk phases of cholesteryl oleate, possibly as a consequence of the constraints of the droplet boundaries. Bright-field illumination shows that the droplets maintain their spherical shape throughout the temperature range observed (25–50°C).

phases and mesophases. Each of the four physical states of the esters in bulk phases could be distinguished under the microscope. During scans through the smectic-cholesteric phase transition, the birefringent pattern of one mesophase disappeared, the field darkened, and the birefringent pattern of the other mesophase emerged. The smectic-cholesteric transition temperatures of these esters were measured and are reported in Table II.

A mixture of cholesteryl ester, phospholipid, and water was sonicated to produce a suspension of cholesteryl ester droplets stabilized by an outer layer of

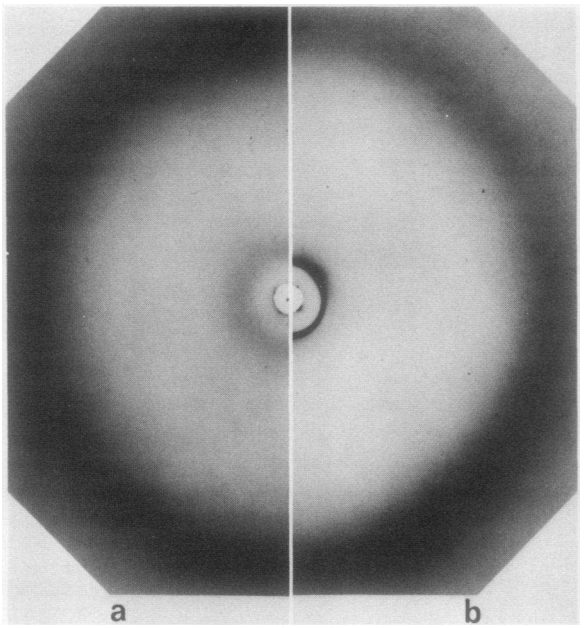

FIGURE 5 Diffraction from cholesteryl oleate. Pure cholesteryl oleate was sealed in a glass capillary and its diffraction pattern recorded as a function of temperature. The patterns shown extend from (100 Å)$^{-1}$ equivalent Bragg spacing (near the beam stop) to about (4 Å)$^{-1}$ at the edge of the photo. (*a*) 60°C. Here two broad bands are evident, an inner one at about (30 Å)$^{-1}$, and a strong outer band centered at about (5 Å)$^{-1}$. This is the liquid state of cholesteryl oleate, and we interpret the bands as arising from end-to-end and side-to-side correlations of the elongated cholesteryl oleate molecules; however, the actual magnitudes of the spacings must be regarded as only very approximate indications of the actual intermolecular spacings involved. (*b*) 37°C. The broad band near (5 Å)$^{-1}$ is like that of the liquid, but the broad band at (30 Å)$^{-1}$ is replaced by a strong, sharp reflection at (34 Å)$^{-1}$. This is the smectic phase of cholesteryl oleate, in which the molecules are arrayed in layers which are spaced regularly at 34-Å intervals. In the plane of each layer, the molecules are still liquid-like, however, as shown by the wide-angle scattering from their side-to-side correlations. The central line is vastly overexposed to bring the scattering band at (5 Å)$^{-1}$ to an intensity comparable to that in Fig.. 3*a*.

phospholipid layer.[3] At temperatures corresponding to the smectic phase, the droplets exhibited the formée cross and the positive sign of birefringence (Fig. 3). Occasionally a large droplet exhibited an apparent negative sign of birefringence while all the surrounding smaller droplets (all the droplets consist of the same cholesteryl ester) exhibited the positive sign. The discrepancy illustrates a limitation of reliance on birefringent sign to identify physical states of cholesteryl esters. Whereas the color scheme of the smaller, positively signed birefringent droplets arises from first-and-second-order interference with the quarter-wave-length plate, the color scheme of the negatively signed birefringent droplet arises from higher-order interference. That is, the larger droplet presents a longer path length to passing light and thus, higher-order interference patterns are observed. When droplets were heated to temperatures corresponding to the cholesteric state, they remained birefringent but no longer exhibited the formée cross. Instead, several irregularly shaped birefringent domains appear within each droplet and these domains did not exhibit any apparent birefringent sign (see Fig. 4).

Cholesteryl myristate is enantiotropic and each of its phase transitions is reversible. Cholesteryl oleate and cholesteryl linoleate are monotropic. For these esters the smectic-to-crystalline transition is irreversible; that is, the crystalline state melts directly to the isotropic liquid state. On cooling, the liquid undergoes three phase transitions, first, to the liquid-crystalline cholesteric mesophase, then to the liquid-crystalline smectic mesophase, and finally to the crystalline phase. The first two of these phase transitions are reversible.

The crystalline states, the mesophases, and the isotropic liquid phases of these esters were also studied by X-ray diffraction. Transition temperatures were identified as that temperature at which one phase pattern disappeared and another emerged. The melting temperatures from the smectic state are also reported in Table II for these esters. The mesophase diffraction patterns for cholesteryl oleate are shown in Fig. 5.

The smectic mesophase patterns exhibited a single, sharp low-angle reflection and a broad (5.0 Å)$^{-1}$ band for each ester. The peak intensity of the low-angle reflection was about 50 times more intense than that of the (5 Å)$^{-1}$ band (1). The low-angle reflection was at an equivalent first-order Bragg spacing of (33.5 Å)$^{-1}$ for cholesteryl linoleate. No other Bragg reflections were observed in the range from (3 Å)$^{-1}$ to (300 Å)$^{-1}$.

When the temperature was raised to the smectic-cholesteric melting point, the low-angle line suddenly broadened and lost much of its peak intensity. The peak of the broadened line was shifted slightly outwards [about (0.5 Å)$^{-1}$] to a smaller equivalent Bragg spacing. This is the cholesteric pattern. The low-angle peak broadened slightly as the temperature was raised into the range of an isotropic liquid. The changes in the diffraction pattern were too subtle to form the basis of a distinction between the cholesteric and liquid phases of fatty streak material, where the diffuse background scatter obscured the diffuse inner ring (see Fig. 2*a*).

DISCUSSION

Material containing fatty streaks gives a strong Bragg reflection while material lacking visible fatty streaks

[3] By a procedure suggested by G. G. Shipley in a personal communication.

does not. The primary difference between these two materials is the accumulation of cholesteryl ester droplets in the lesions. The diffraction pattern observed for pure cholesteryl esters in the smectic liquid-crystalline state are similar to those observed for the fatty streak material. Furthermore, the range of melting temperatures embraced by those of cholesteryl oleate and cholesteryl linoleate, the primary esters in the lesion, is similar to the melting range observed with X-ray diffraction of the fatty streak material. The results of Krzewski and Porter (17) show that mixtures of cholesteryl esters have properties intermediate between those of the two pure compounds. These observations combine to show that the reflection from the lesion is due to the organization of cholesteryl esters into a smectic phase, and that the thermotropic disappearance of the reflection arises from an order-to-disorder phase transition. The fact that we cannot differentiate between the nematic, the cholesteric, and the isotropic liquid phase by X-ray diffraction prevents us from specifying which phase derives from the smectic phase as it melts.

Using polarized light microscopy, Hata et al. (7) observed the formée cross in spherulites from atherosclerotic lesions, determined that they exhibited the positive sign of birefringence, and concluded that the organization of the constituents within such a sperulite was radially symmetric. Although Hata et al. proposed that the droplets were in a smectic state, they acknowledged the tentative nature of this conclusion. The property of the droplets actually demonstrated by the application of polarized light microscopy is the radially enhanced polarizability within the ester droplets. It then must be argued that cholesteryl ester molecules (particularly if in the extended configuration) are likely to have enhanced polarizability in the direction of their long axes, a reasonable presumption from the known properties of elongated molecules. Therefore, for the droplets to exhibit the formée cross and have a positive sign, there must be a net radial component of orientation of the cholesteryl ester molecules in the droplet.

This organization could be either a smectic or a radial nematic phase (see (Fig. 1) and one cannot differentiate between these two states using polarized light alone. Hata et al. argued that the droplets cannot exist as nematic phases, since cholesteryl esters are not found in such phases when studied in planar or bulk systems; however, the constraint of a spherical droplet may alter the organization. Hata et al. have put forward a second argument, that the smectic model is the correct organization in the droplet, based on the existence of 27 Å-thick electron-dense lamellae in dried, fixed specimens viewed at an unknown temperature in the electron microscope; however, no such structure is reported in the paper (18) cited by Hata et al., although a 55 Å periodicity is reported. In any case, this type of observation is of questionable relevance to the structure of the droplets in vivo, since cholesteryl ester mesophases are thermotropic and the spherical shape of the droplet is most likely maintained by hydrophobic interactions. Conclusions based on the above arguments must therefore be regarded as tenuous. Thus the additional information revealed by X-ray diffraction was necessary to specify unambiguously the molecular organization in birefringent droplets.

The only birefringent material observed in the fatty streak tissue were the droplets. We conclude that a significant proportion of the birefringent droplets observed microscopically in fatty streak material (3–6) consists of cholesteryl esters organized in the smectic phase. From our information, combined with the conclusions of Hata et al. that the organization is radial and symmetric, the most probable organization is that the layers of the smectic phase form concentric shells, wrapped one over another like the layers of an onion (Fig. 1). Each lamella is a thin shell wrapped around the surface of a sphere, rather than a flat plane. In a shell with a large radius of curvature, the neighborhood around an individual molecule will appear planar. Towards the center of the droplet the curvature may be too large for the smectic state to exist in shells, so that the droplet center may be somewhat disorganized or even filled with solvent; however, the existence of smectic organization in lipoproteins shows that regions of less than 200 Å may be in the smectic state (19). Such a structure would have the necessary geometrical symmetry to exhibit a formée cross under polarized light.

Unforunately, the details of the molecular conformation are not derivable from the current data. Measurements of Corey, Pauling, and Koltun models give a value of 37.4 Å for the length of a fully extended molecule of cholesteryl myristate (20). From observations of cholesteryl myristate oriented in a capillary, it was shown that the $(5\ \text{Å})^{-1}$ peak arises from an organization whose repeat vectors are roughly perpendicular to the repeat vectors of the lattice giving rise to the $(33.4\ \text{Å})^{-1}$ peak (1). These data suggest two possible models for the molecular arrangement in the lamella. The 37-Å-long molecules could be tilted to fit into the 33.5-Å-thick lamellae. Alternatively, the molecules could be bent over at the ester linkage, tilted, and packed in a bilayer arrangement. With only one Bragg reflection it is difficult to discern the correct arrangement. The absence of higher orders may be due to thermal disorder (21) or it is possible that the electron density function is well represented as a sine wave to moderate resolution so that the Fourier transform of the layer has low values over an extended region after the first order. We have not been satisfied with any of our

model-building attempts to explain the implied electron density distribution except in terms of great thermal disorder. However, the use of specific deuteration and neutron scattering should permit us to establish whether the esters are folded or extended in the smectic lamellae (22). Finally, for both models the broad (5 Å)$^{-1}$ band arises from the side-to-side liquid-like packing of the molecules in the plane of the lamella.

It is important to discuss some apparent discrepancies between the synthetic model studies and the fatty streak material studies. A (5 Å)$^{-1}$ diffuse band is observed in diffraction patterns from pure, synthetic cholesteryl esters in the smectic A, cholesteric, and isotropic-liquid phases. The band is not observed above the background in diffraction patterns from fatty streak material. The failure to observe the (5 Å)$^{-1}$ band in early fatty streak material arises from the weakness of the (5 Å)$^{-1}$ band, the low concentration of lipid droplets in the tissue, and the large amount of diffuse scattering from other structures (e.g., proteins) in the region of the band. For pure cholesteryl esters in the smectic A state, the (5 Å)$^{-1}$ band was 50 times weaker in peak intensity than the (36 Å)$^{-1}$ reflection (Fig. 3). The low concentration of lipid droplets is demonstrated by the time required to obtain a well-exposed picture of the low-angle peak. For intima-media preparations it was 24 h; for pure cholesteryl esters it was only 4 h. In patterns obtained from aortic material, there was a diffuse band centered between (10 Å)$^{-1}$ and (14 Å)$^{-1}$, and there was diffuse scatter beginning at about (5.5 Å)$^{-1}$ and extending to the edge of the film, [(3 Å)$^{-1}$]. These diffuse bands arose from other structures in the tissue. Proteins typically have diffraction peaks in the (10–12 Å)$^{-1}$ region and the (4–5 Å)$^{-1}$ region. Lipids in the fluid state have a broad diffraction peak centered at (4.6 Å)$^{-1}$. Water diffracts in a broad region centered about (3.3 Å)$^{-1}$. Proteins, membrane lipids, and water constitute the bulk of the intima-media preparation. The difficulty in observing the (5 Å)$^{-1}$ band is basically a signal-to-noise problem. The weak (5 Å)$^{-1}$ band is obscured by the background.

The spacing of the low-angle peak ranged from (32.2 Å)$^{-1}$ to (36.8 Å)$^{-1}$ and the mean spacing was (35.6 Å)$^{-1}$ with a standard deviation of (1.0 Å)$^{-1}$. The cholesteryl ester fatty acid composition of isolated lipid droplets shows that the droplets consist of many esters (4). Our X-ray diffraction studies on pure synthetic cholesteryl esters revealed that the low-angle reflections for smectic A cholesteryl myristate, cholesteryl oleate, and cholesteryl linoleate corresponded to equivalent Bragg spacings of (33.5 Å)$^{-1}$, (34 Å)$^{-1}$, and (35 Å)$^{-1}$. Furthermore, the spacings of smectic cholesteryl myristate were found to be temperature-dependent, ranging from (33.95 Å)$^{-1}$ at 63.5°C to (33.20 Å)$^{-1}$ at 77.6°C (20). The thickness of the smectic layer, which corresponds to the low-angle spacing, may arise as an average property of the molecular mixture in the droplets.

The range in transition temperatures observed in the atherosclerotic material was from 28°C to 42°C, which probably arises from the compositional variability of the droplets. The binary phase diagram between cholesteryl oleate and cholesteryl linoleate has revealed that the smectic-to-cholesteric transition temperature is a linear function of molar composition and ranges from 32.6°C to 39.3°C (17). If many cholesteryl esters contribute to determine the transition temperature, the experimentally observed range could easily be explained. For instance, cholesteryl palmitate and cholesteryl linolenate melt from the smectic state at 76° and 27°C.

Another aspect of the melting behavior of the atherosclerotic material concerns the width of the transition. The low-angle line intensity decreased over a temperature range of about 5–10°C upon heating, whereas the synthetic esters melted sharply from the smectic phase within 0.5°. The problem is as follows: Fatty streak material contains many cholesteryl ester droplets. The X-ray beam records an average spacing and melting temperature for the population. A mixture of several cholesteryl esters could exhibit a wide melting transition or, alternatively, the wide melt could arise from droplets melting sharply but at different temperatures. This issue is investigated in a separate paper, which establishes that the second alternative applies (15).

It has been suggested by Small (23) that the constraints of the viscosity and orienting forces in mesophases may influence the accumlation of cholesteryl esters. Our present study permits a refinement of this general notion to include more specific molecular considerations. A molecule in the smectic phase will expose only a small portion of itself at the lamellar surface and this small portion will not represent all regions of its structure. For instance, if a cholesteryl ester were in its extended form in the smectic layer, then the hydrocarbon tail end of the cholesterol moiety, or the methyl end of the fatty acid moiety or both ends would be exposed to the surroundings at the outer surface of the outermost lamella. However, the ester linkage between the cholesterol and the fatty acid would be buried in the center of the lamella. The smectic organization may well restrict the accessibility of enzymes to this linkage for either metabolism or transport. This would not be the case for the less-ordered cholesteric and liquid phase droplets. Here all parts of any molecule could be exposed at the droplet-water interface at various times and a wide range of enzyme-substrate contacts would be possible. Thus

the phase of the esters may be important in the mechanisms for the persistence of the lipid deposits.

ACKNOWLEDGMENTS

We wish to thank Ms. B. Gillette for her help in the polarized light microscopic studies of the synthetic esters and Mr. B. Orland for his help in the lipid analysis. We are indebted to Dr. L. L. Waters of the Yale Medical School for his useful advice and criticism of this work. This study was supported by a grant from the National Heart and Lung Institute (Hl 414111).

REFERENCES

1. Hillman, G. M. 1975. Thermotropic states of lipid deposits in human atherosclerotic fatty streak lesions. Ph.D. Thesis. Yale University, New Haven, Conn. Available from University Microfilms, Ann Arbor, Mich.
2. Hillman, G., and D. M. Engelman. 1974. A lipid phase transition in human atherosclerotic lesions. *Fed. Proc.* **33**: 1327. (Abstr.)
3. Small, D. M., and G. G. Shipley. 1974. Physical-chemical basis of lipid deposition in atherosclerosis. The physical state of the lipids helps to explain lipid deposition and lesion reversal in atherosclerosis. *Science (Wash. D.C.).* **185**: 222–229.
4. Lang, P. D., and W. Insull, Jr. 1970. Lipid droplets in atherosclerotic fatty streaks of human aorta. *J. Clin. Invest.* **49**: 1479–1488.
5. Kaiserling, C., and A. Orgler. 1902. Über das Auftreten von Myelin in Zellen und seine Beziehung zur Fettmetamorphose. *Virchows Arch. A Pathol. Anat. Histol.* **167**: 296–310.
6. Stewart, G. T. 1959. Liquid crystals of lipide in normal and atheromatous tissue. *Nature (Lond.).* **183**: 873–875.
7. Hata, Y., J. Hower, and W. Insull, Jr. 1974. Cholesteryl ester-rich inclusions from human aortic fatty streak and fibrous plaque lesions of atherosclerosis. I. Crystalline properties, size and internal structure. *Am. J. Pathol.* **75**: 423–456.
8. Fergason, J. L. 1964. Liquid crystals. *Sci. Am.* **211** (August): 77–85.
9. Gray, G. W. 1962. Molecular Structure and Properties of Liquid Crystals. Academic Press, Inc., New York. 17–55.
10. Gould, S. 1973. Atherosclerosis: A Primer for Scientists. Polyscience Monographs, New York. 5–11.
11. Putt, F. A. 1956. Flaming red as a dye for the demonstration of lipids. *Lab. Invest.* **5**: 377–379.
12. Elliott, A. 1965. The use of toroidal reflection surfaces in x-ray diffraction cameras. *J. Sci. Instrum.* **42**: 312–316.
13. Franks, A. 1958. Some developments and applications of microfocus x-ray diffraction techniques. *Br. J. Appl. Phys.* **9**: 349–352.
14. Morrison, W. R., and L. M. Smith. 1964. Preparation of fatty acid methyl esters and dimethylacetals from lipids with boron fluoride-methanol. *J. Lipid Res.* **5**: 600–608.
15. Hillman, G. M., and D. M. Engelman. 1976. Compositional mapping of cholesteryl ester droplets in the fatty streaks of human aorta. *J. Clin. Invest.* **58**: 1008–1018.
16. Guinier, A. 1963. X-ray Diffraction. W. H. Freeman and Company, Publishers, San Francisco, Calif.
17. Krzewki, R. J., and R. S. Porter. 1973. Phase studies on binary systems of cholesteryl esters: Three C_{18} ester pairs. *Mol. Cryst. Liq. Cryst.* **21**: 99–124.
18. Weller, R. O., R. A. Clark, and W. B. Oswald. 1968. Stages in the formation and metabolism of intracellular lipid droplets in atherosclerosis. An electron microscopical and biochemical study. *J. Atheroscler. Res.* **8**: 249–263.
19. Deckelbaum, R. J., G. G. Shipley, D. M. Small, R. S. Lees, and P. K. George. 1975. Thermal transitions in human plasma low density lipoproteins. *Science (Wash. D. C.).* **190**: 392–394.
20. Wendorff, J. H., and F. P. Price. 1974. The structure of mesophases of cholesteryl esters. *Mol. Cryst. Liq. Cryst.* **27**: 129–144.
21. McMillan, W. L. 1972. X-ray scattering from liquid crystals. I. Cholesteryl nonanoate and myristate. *Phys. Rev. A* **6**: 936–947.
22. Engelman, D. M., and P. B. Moore. 1975. Determination of quaternary structure by small angle neutron scattering. *Annu. Rev. Biophys. Bioeng.* **4**: 219–241.
23. Small, D. M. 1970. The physical state of lipids of biological importance: cholesteryl esters, cholesterol, triglyceride. *In* Surface Chemistry of Biological Systems. M. Blank, editor. Plenum Publishing Corporation, New York. 55–82.